ACS OMEGA

Open Access

http://pubs.acs.org/journal/acsodf

Article

"Alkyl-Substituted Phenoxy" Spacer Strategy: Antiaggregated and Highly Soluble Zinc Phthalocyanines for Color Films

Shi Li, Yong Qi, Jiahui Wang, Wenbin Niu, Wei Ma, Bingtao Tang, and Shufen Zhang*

Cite This: *ACS Omega* 2024, 9, 50774−50785

Read Online

ACCESS | Metrics & More | Article Recommendations | Supporting Information

ABSTRACT: A series of zinc phthalocyanine derivatives (ZnPcs) were designed by introducing different volumes of steric hindrance groups (chlorine atom, n-propyloxy, isopropyloxy, n-butoxy, isobutoxy, *tert*-butoxy, 2,4-di-*tert*-butylphenoxy, 2,4-di-*tert*-pentylphenoxy) on the peripheral and nonperipheral positions of phthalocyanine. Density functional theory (DFT) calculations presented that the substitution of sterically hindered 2,4-di-*tert*-butylphenoxy or 2,4-di-*tert*-pentylphenoxy on the peripheral positions effectively reduced the aggregation of ZnPcs, improving the solubility of ZnPcs, and the simultaneous substitution on the peripheral and nonperipheral positions could achieve ZnPcs with different colors. From the calculation results, six low-aggregation ZnPcs were synthesized for the first time. The solubilities of the synthesized ZnPcs are above 6.0/100 g. Furthermore, their color films displayed excellent transmittance because of the introduction of sterically hindered 2,4-di-*tert*-butoxyphenoxy or 2,4-di-*tert*-pentylphenoxy moieties. Also, the color films exhibit great photo and thermal stability (ΔE < 3).

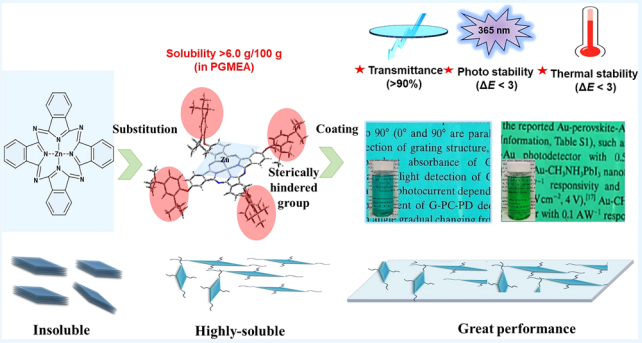

1. INTRODUCTION

Phthalocyanine derivatives (Pcs) are aromatic heterocyclic dyes containing 18 delocalized π-electrons and a central cavity approximately 2.7 Å in diameter.[1−3] Due to their high molar absorption coefficient,[4,5] strong electron affinities, and brilliant color,[6,7] they are not only recognized as classical dyes in practical applications[8] but also as modern functional materials in various fields, including semiconductors,[9] solar cells,[10] gas sensors,[11] optical data storage devices,[12] liquid crystals, and photosensitizers in photodynamic therapy.[13,14] However, unsubstituted phthalocyanines often form $\pi-\pi$ stacking between molecules, causing aggregation and poor solubility in organic solvents or water. This aggregation can reduce the photophysical properties of Pcs,[15−17] thus limiting their practical applications in devices.

A common strategy to reduce aggregation of Pcs is introducing metal atoms at the center of the phthalocyanine (M position) (see Figure 1) to regulate the planar conformation through metal coordination bonds to prevent $\pi-\pi$ stacking effects in the phthalocyanine chromophore.[17] For example, metal atoms like titanium and magnesium were introduced into the phthalocyanine,[18−30] and the coordination bond between the metal atoms and the phthalocyanine led to the decline in planarity of the molecule and the tendency of $\pi-\pi$ stacking in solution. Among those metal phthalocyanines, zinc phthalocyanine derivatives (ZnPcs) show a more positive charge on the center of the phthalocyanine due to the lower electronegativity of Zn, leading to the higher electric

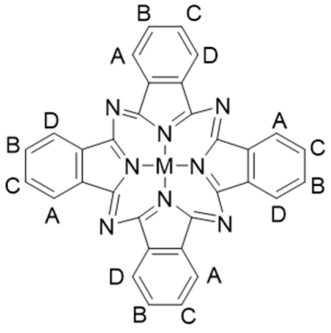

Figure 1. General structure of the Pcs.

polarizability for ZnPcs and reducing the intermolecular aggregation.[19,20] In addition, the stability of ZnPcs gets great improvement by the formation of two covalent bonds and two coordination bonds at the cavity position between zinc and phthalocyanine.[19−21]

Another widely used strategy to mitigate the aggregation of phthalocyanines (Pcs) involves substitution at their peripheral

Received: October 9, 2024
Revised: November 28, 2024
Accepted: December 3, 2024
Published: December 12, 2024

(B, C positions) and nonperipheral (A, D positions) sites (see Figure 1).[21] This modification disrupts the planarity of the Pcs, effectively reducing intermolecular $\pi-\pi$ stacking interactions.[22,23] In addition, the peripheral and nonperipheral position substitution not only decreases aggregation by disrupting planarity but also significantly alters their absorbance characteristics, leading to intriguing photophysical properties.[24] For example, simultaneous modification of Pcs' A, B and C, D positions by multiple chlorine atoms and bulky substituents decorated with two methoxy groups reduces the planarity of the Pcs, as well as changes in the conjugation system, leading to a significant red shift of the molecule's absorption, resulting in novel green Pcs. However, the molar absorption coefficient of phthalocyanine dyes was seriously weakened by the introduction of excessive molecular weight substituents, resulting in the decrease of brightness for color films.[25−29] Notably, the introduction of *tert*-butyl groups at the B and C positions of the phthalocyanine ring reduced the intermolecular distance, resulting in the formation of a novel type of cyan phthalocyanines (Pcs). The obtained Pcs had higher fluorescence quantum yields than the unmodified molecules in the pure films,[29−33] reflecting the improved solubility and high molar absorption coefficient of Pcs by *tert*-butyl group. In spite of these successes, some constraints remain: (1) the distance between individual molecules gets improved by incorporation of the *tert*-butyl group, but the coplanarity of the Pcs is still high, which leads to aggregate under the solution with high concentration; (2) the poor solubility limits further solution processing and preparation of color film.

Herein, a series of zinc phthalocyanine derivatives (ZnPcs) substituted with chlorine and alkyl-substituted phenoxy groups were designed and simulated using the Gaussian 16 program. The aim was to theoretically analyze the impact of sterically hindered group volumes on the molecular vertical axial bulkiness, dihedral angles, and absorption spectra of ZnPc dyes. Based on the simulation results, six ZnPc dyes exhibiting representative values for vertical axial bulkiness and dihedral angle were selected to investigate the correlation between their molecular structures and solubility in PGMEA, as well as their photophysical properties in both solution and solid states. Furthermore, to evaluate the practicality of the synthesized ZnPc dyes, the corresponding color films were prepared using a spin-coating process. The properties of these films were investigated to enhance the antiaggregation behavior, as well as the photostability and thermal stability of the phthalocyanine dyes in color films.

2. EXPERIMENTAL SECTION

2.1. Materials and Instruments. *N*-Methyl pyrrolidone (NMP), 4-nitrophthalonitrile, 4,5-dichlorophthalonitrile, cesium carbonate (Cs_2CO_3), 2,4-di-*tert*-butylphenol, 2,4-di-*tert*-pentylphenol, propylene glycol monomethyl ether acetate (PGMEA), and polysulfone (PSU, M_w = 80,000) were purchased from Sigma-Aldrich.

The analysis of the prepared zinc phthalocyanine derivatives (ZnPcs) was conducted by employing a suite of analytical instruments. Nuclear magnetic resonance (NMR) spectra, specifically the ^{1}H NMR, were documented on a Bruker Avance III 400 MHz system with tetramethylsilane (TMS) as an internal reference, whereas the ^{13}C NMR spectra were captured on the same model's 600 MHz setup, also utilizing TMS. Mass determination of the ZnPc derivatives was accomplished through MALDI-TOF mass spectrometry. Infrared spectra were registered on a Jasco FTIR-430 device with potassium bromide (KBr) pellets. Thermogravimetric analysis (TGA) was conducted in a nitrogen environment at a ramp rate of 10 °C/min using a TGA Q500 apparatus. Absorption spectra in the ultraviolet−visible region were recorded with an Agilent 8453 spectrophotometer. Film fabrication was achieved by spin-coating the ZnPc solution onto a transparent glass substrate by employing a MIDAS SPIN-1200D device. The transmittance spectra of the ZnPc dye-based films were quantified before and after irradiation using a U-4100 spectrophotometer.[30]

2.2. Geometric Optimization of the Designed Zinc Phthalocyanine Derivatives (ZnPcs). The synthesis of phthalocyanines involved the incorporation of chlorine and various substituents, such as alkoxy and alkyl-substituted phenoxy, at the peripheral sites of the phthalocyanine macrocycle. Phthalocyanines with alkoxy or alkyl-substituted phenoxy modifications at peripheral sites were further functionalized with varying quantities of chlorine at nonperipheral sites to synthesize novel ZnPc dyes. The structural characterization and theoretical determination of their absorption were performed by employing the B_3LYP functional with Cam-B_3LYP basis sets in Gaussian 16 software. The dihedral angle between the substituents and the plane of the isoindole ring in the ZnPc dyes was extracted from the optimized geometric structures. Additionally, the molecular bulkiness along the axial direction (for C-1a to C-7a, C-1b to C-7b, and C-1c to C-7c) and the volume of various groups, including n-propyloxy, isopropyloxy, n-butyloxy, isobutoxy, *tert*-butyloxy, 2,4-di-*tert*-butylphenoxy, and 2,4-di-*tert*-pentylphenoxy, were computationally assessed.

2.3. Synthesis. *2.3.1. Synthesis of the Compound 6a.* For the synthesis of compound 6a, the reactants included 4-nitrophthalonitrile (7.0 g, 0.04 mol), cesium carbonate (Cs_2CO_3, 15.6 g, 0.046 mol) in an anhydrous form, and 2,4-di-*tert*-butylphenol (9.5 g, 0.046 mol). They were mixed in anhydrous dimethylformamide (DMF, 120 mL), and the resulting suspension was heated to 80 °C for 12 h. After the reaction was complete, the mixture was cooled in an ice bath and then filtered over ice to yield a powdery crude product. The crude product was purified using column chromatography with a 1:1 ethyl acetate to petroleum ether eluent, yielding compound 6a with an R_f of 0.79 and 97% yield.

2.3.2. Synthesis of Compound 7a. For the synthesis of compound 7a, the ingredients comprised 4-nitrophthalonitrile (7.0 g, 0.04 mol), arid cesium carbonate (Cs_2CO_3, 15.6 g, 0.046 mol), and 2,4-di-*tert*-pentylphenol (9.6 g, 0.046 mol). They were combined in anhydrous dimethylformamide (DMF, 120 mL) and heated to 80 °C for 12 h. After the reaction, the mixture was cooled in an ice bath, and then the precipitate was collected by filtration through an ice-water medium (80 mL), yielding a powdery residue. The residue was refined via column chromatography with a 1:1 ratio of ethyl acetate to petroleum ether as the eluent, leading to the acquisition of compound 7a with an R_f value of 0.79 and a 95% yield.

2.3.3. Synthesis of Compound 6b. For the synthesis of compound 6b, the utilized reactants included 4,5-dichlorophthalonitrile (7.2 g, 0.04 mol), cesium carbonate devoid of water (Cs_2CO_3, = 15.6 g, 0.046 mol), and 2,4-di-*tert*-butylphenol (9.5 g, 0.046 mol). These components were mixed in anhydrous dimethylformamide (DMF, 120 mL), and the resulting suspension was maintained at 80 °C for 12 h. After

https://doi.org/10.1021/acsomega.4c08931
ACS Omega 2024, 9, 50774−50785

the reaction was completed, the mixture was cooled in an ice bath. The cooled suspension was then filtered through an ice-water medium to yield a powdery crude product. The crude product was further purified by column chromatography using a 1:3 mixture of ethyl acetate and petroleum ether as the the eluent, resulting in a purified compound 6b with an R_f of 0.73 and a 90% yield.[19]

2.3.4. Synthesis of Compound 7b. A variety of substances were employed: 4,5-dichlorophthalonitrile (7.2 g, 0.04 mol), anhydrous cesium carbonate (Cs_2CO_3, 15.6 g, 0.046 mol), and 2,4-di-*tert*-pentylphenol (9.6 g, 0.046 mol). These components were mixed in dry dimethylformamide (DMF, 120 mL) and subjected to heating at 80 °C for a duration of 12 h. Postreaction, the blend was cooled using an ice-water mixture. Subsequently, the mixture was passed through a filtration setup on ice to isolate a granular byproduct. This byproduct was then refined via column chromatography using the eluent of ethyl acetate to petroleum ether in a 1:3 ratio, resulting in the isolation of compound 6a with an R_f value of 0.793 and a yield of 85%.

2.3.5. Synthesis of Compound 6c. For the synthesis of compound 6c, the following ingredients were utilized: 3,4,5,6-tetrachlorophthalonitrile (7.2 g, 0.04 mol), anhydrous cesium carbonate (Cs_2CO_3, 15.6 g, 0.046 mol), and 2,4-di-*tert*-butylphenol (9.5 g, 0.046 mol). These substances were blended in dehydrated dimethylformamide (DMF, 120 mL), and the reaction was warmed to 80 °C for 12 h. Once the reaction was complete, the mixture was cooled in an ice bath. The cooled mixture was then passed through a filtration medium with ice water (80 mL) to precipitate the raw product in a powdered form. The raw powder was further purified using column chromatography with a the eluent of ethyl acetate and petroleum ether in a 1:4 ratio, which resulted in the isolation of the purified product with an R_f value of 0.88 and a yield of 84%.[19]

2.3.6. Synthesis of Compound 7c. In the creation of compound 7c, the following substances were utilized: 3,4,5,6-tetrachlorophthalonitrile (7.2 g, 0.04 mol), anhydrous cesium carbonate (Cs_2CO_3, 15.6 g, 0.046 mol), and 2,4-di-*tert*-pentylphenol (9.6 g, 0.046 mol). These were mixed in anhydrous dimethylformamide (DMF, 120 mL), and the reaction was warmed to 80 °C for 12 h. After the reaction had concluded, the mixture was cooled in an ice bath to lower its temperature. The cooled mixture was then filtered through a medium with ice water (80 mL) to precipitate the raw product in a granular form. The raw granules were purified using column chromatography with a the eluent of ethyl acetate and petroleum ether in a 1:4 ratio, resulting in the pure product with an R_f value of 0.92 and a yield of 86%.[19]

2.3.7. Synthesis of the Designed ZnPc Dye C-6a. Initially, 6a (26.6 g, 0.08 mol, 332 g/mol) and $ZnCl_2$ (2.64 g, 0.08 mol, 136 g/mol) were mixed in 100 mL of 1-pentanol, and the solution was heated to 150 °C. DBU (1.50 g, 0.001 mol, 152 g/mol) was incrementally added, and stirring was continued for 5 h under nitrogen. Upon cooling, the reaction mixture was poured into 100 mL of methanol to precipitate the product. The resulting solid was filtered, dried at 50 °C under vacuum, and then purified by silica gel column chromatography with ethyl acetate as the eluent (R_f = 0.11), resulting in a 77% yield of the purified compound.

2.3.8. Synthesis of the Designed ZnPc Dye C-6b. 6b (27.8 g, 346 g/mol, 0.08 mol) and $ZnCl_2$ (2.64 g, 136 g/mol, 0.08 mol) were combined in 1-pentanol (100 mL) and heated to 150 °C. DBU (1.50 g, 152 g/mol, 0.001 mol) was introduced dropwise, and the mixture was stirred for 5 h under nitrogen. Postreaction, the mixture was cooled, and the crude product was isolated by adding it to methanol (100 mL). The solid was then dried at 50 °C under a vacuum. Purification was achieved through column chromatography on silica gel with ethyl acetate as the eluent, yielding the product with an R_f of 0.12 and an 89%.

2.3.9. Synthesis of the Designed ZnPc Dye C-7a. In the preparation of 7a, the compound (28.8 g, 360 g/mol, 0.08 mol) was combined with $ZnCl_2$ (2.64 g, 136 g/mol, 0.08 mol) in 100 mL of 1-pentanol and the mixture was heated to 150 °C. DBU (1.50 g, 152 g/mol, 0.001 mol) was introduced drop by drop, and the solution was agitated for 5 h under nitrogen. Postcooling, the mixture was transferred to 100 mL of methanol to induce precipitation. The precipitated solid was then dried under vacuum at 50 °C. Purification of the product was achieved through column chromatography on silica gel with ethyl acetate as the eluent (R_f = 0.12), resulting in an 89% yield.

2.3.10. Synthesis of the Designed ZnPc Dye C-7b. 29.6 g (374 g/mol, 0.08 mol) of 7b and 2.64 g (136 g/mol, 0.08 mol) of $ZnCl_2$ were dissolved in 100 mL of 1-pentanol, and the solution was heated to 150 °C. DBU (1.50 g, 152 g/mol, 0.001 mol) was incrementally added, and the mixture was stirred for 5 h under nitrogen. Upon cooling, the reaction was quenched by adding the mixture to 100 mL of methanol to form a precipitate. The precipitate was then dried under vacuum at 50 °C. The purification process involved silica gel column chromatography with ethyl acetate as the eluent, yielding a final product with an R_f of 0.12 and an 88% yield.

2.3.11. Synthesis of the Designed ZnPc Dye C-6c. 29.6 g (374 g/mol, 0.08 mol) of 6c and 2.64 g (136 g/mol, 0.08 mol) of $ZnCl_2$ were combined in 100 mL of 1-pentanol, and the temperature was raised to 150 °C. DBU (1.50 g, 152 g/mol, 0.001 mol) was introduced gradually, and the mixture was agitated for 5 h under nitrogen. Once cooled, the crude product was formed by adding the mixture to 100 mL of methanol. The resulting solid was then vacuum-dried at 50 °C. Purification was conducted via silica gel column chromatography with a 1:3 ethyl acetate to petroleum ether solvent system, achieving an R_f of 0.25 and a 69% yield of the purified product.

2.3.12. Synthesis of the Designed ZnPc Dye C-7c. A quantity of 33.6 g (molar mass 402 g/mol, 0.08 mol) of compound 7c and 2.64 g (molar mass 136 g/mol, 0.08 mol) of zinc chloride were combined in a solution of 100 mL of 1-pentanol, and the solution was warmed to 150 °C. Dibutylamine (DBU, 1.50 g, molar mass 152 g/mol, 0.01 mol) was gradually added, and the mixture was agitated for 5 h in an atmosphere of nitrogen. Upon cooling, the crude product was caused to precipitate by mixing the solution with 100 mL of methanol. The precipitated solid was then dried under vacuum at 50 °C. The purification process involved silica gel column chromatography using the eluent of ethyl acetate to petroleum ether in a 1:3 ratio, which resulted in an R_f value of 0.25 and a yield of 77% for the purified product.

2.4. UV−vis Absorption Spectra of the Synthesized ZnPc Dyes. A solution with the synthesized ZnPc derivatives in PGMEA was formulated. The molar extinction coefficients for these ZnPc dyes were determined using the Lambert−Beer law, as shown in eq 1

https://doi.org/10.1021/acsomega.4c08931
ACS Omega 2024, 9, 50774−50785

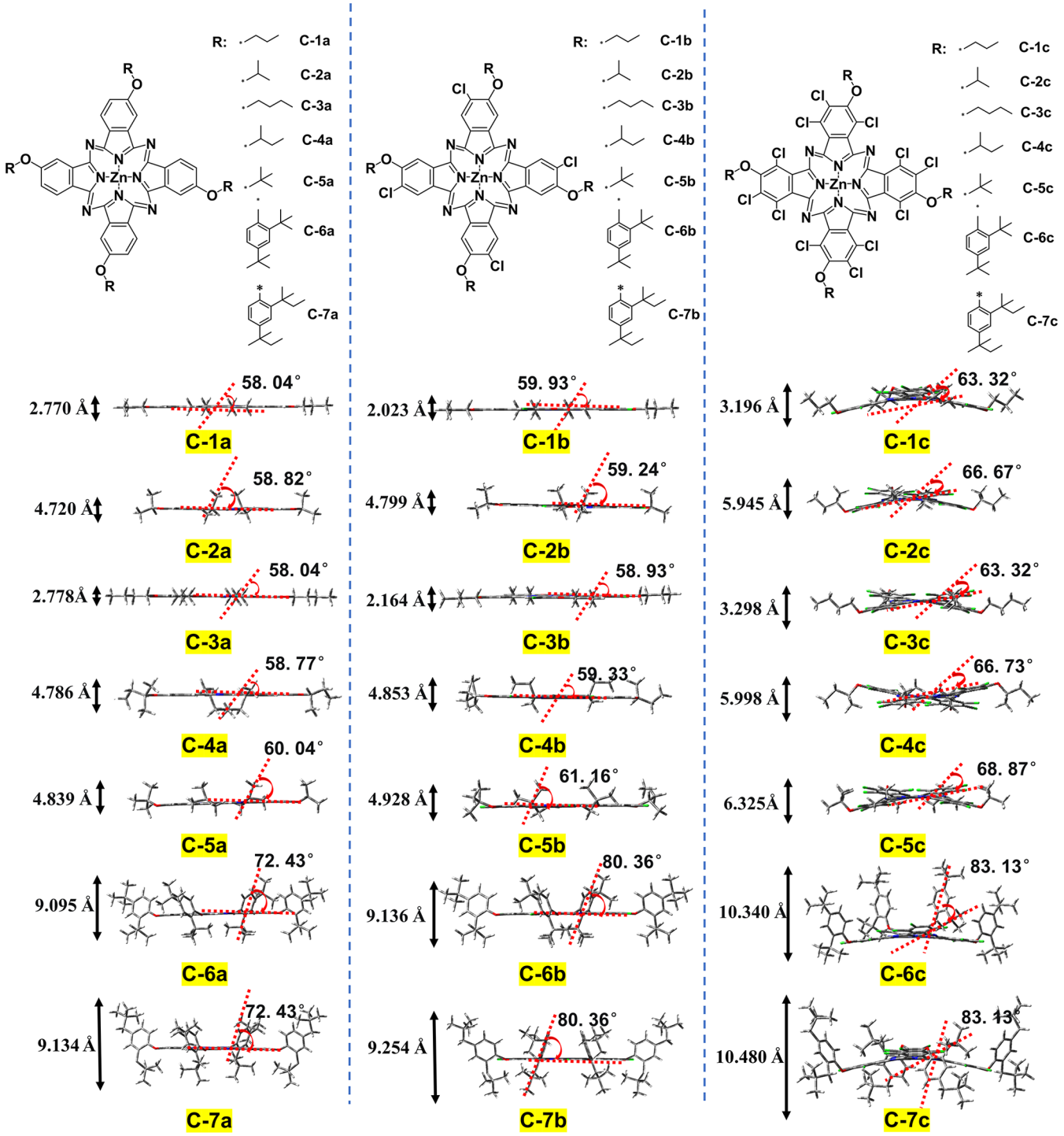

Figure 2. Geometrically optimized structure of the designed ZnPc dyes (dihedral angle of the plane of substituents to the ZnPcs' isoindole ring plane).

$$A = \varepsilon dc \quad (1)$$

where A is the absorbance intensity, ε is the molar absorption coefficient ($L \cdot mol^{-1} \cdot cm^{-1}$), c is the concentration of the solutions ($mol \cdot L^{-1}$), and d is the thickness of the cuvette (cm).

2.5. Determination of the Solubility of the Synthesized ZnPcs in PGMEA. ZnPc dyes weighing 15 g were mixed with PGMEA (100 g) at a temperature of 25 °C to form a solution. This solution underwent sonication for 10 min and was then allowed to settle for 48 h. Following triple filtration, the weight of the filtrate was recorded on an accurate analytical scale. The filtrate was subsequently evaporated in a vacuum oven at 80 °C and a pressure of 2.7 Pa for 7 days. The mass of the leftover solid was also measured using the same scale. The dye's solubility at 25 °C was then computed employing a designated formula.[30]

$$S = \frac{100 m_{\text{residue}}}{m_{\text{filtrate}} - m_{\text{residue}}} \quad (2)$$

2.6. Preparation of the Synthesized ZnPc Dye-Based PSU Films. The ZnPc dispersion was formulated by

https://doi.org/10.1021/acsomega.4c08931
ACS Omega 2024, 9, 50774−50785

integrating 0.005 g of synthesized ZnPc dyes and 0.40 g of PSU binder into 50 g of PGMEA. This mixture was applied onto a clear glass slide via a spin-coater operating at 500 rpm for a duration of 20 s. The resultant ZnPc-based films were subjected to thermal treatment at 80 °C for 20 min, followed by a higher temperature of 200 °C for 60 min. Post each drying phase, the chromatic attributes of the films were quantified using an advanced colorimeter. The proportion of ZnPc dyes in the films was approximately 1.25% by weight.[30]

2.7. Thermal Stability Measurement for the Synthesized ZnPc Dyes. The heat resistance of the synthesized ZnPc dyes was evaluated through thermogravimetric analysis (TGA). Initially, the dye sample was heated to 230 °C for 30 min to mimic the conditions encountered during the production of color films, after which the temperature was elevated to 350 °C to determine the onset of thermal breakdown. The temperature was increased at a rate of 10 °C per minute in a nitrogen atmosphere devoid of oxygen.[30]

2.8. Determination of Thermal Stability and Photostability of the Synthesized ZnPc Dye-Based Color Films. The color difference (ΔE) of the films was measured before and after being baked at 230 °C. The films' resilience to light-induced deterioration was tested by subjecting them to a 365 nm LED light source. The intensity of the ZnPc-based films was set to 20 mW·cm^{-2} by adjusting the distance from the light source, followed by a 5 min illumination period. The spectral transmission of the ZnPc-based films was documented with a spectrophotometer both before and after exposure, and the ΔE values were calculated, respectively. It is anticipated that these films will retain their properties over a long duration under typical conditions. The ΔE values for the dyes were derived by using eq 3.

$$\Delta E = [(\Delta a)^2 + (\Delta b)^2 + (\Delta L)^2]^{1/2} \quad (3)$$

Within the equation, L signifies the luminance, a signifies the chromatic coordinate along the red-green axis, and b denotes the chromatic coordinate along the yellow-blue axis. The color difference, denoted as ΔE, is categorized based on the following criteria: $\Delta E \leq 1$ suggests negligible variation; $1 < \Delta E \leq 2$ implies a minimal perceptible change; $2 < \Delta E \leq 3.5$ signifies moderate divergence; $3.5 < \Delta E \leq 6$ indicates a significant discrepancy; and $\Delta E > 6$ denotes a substantial difference.[1]

3. RESULTS AND DISCUSSION

3.1. Geometry Optimization and TD-DFT Calculations of the ZnPc Dyes. As mentioned above, nonperipheral (A, D) and peripheral (B, C) substituents in phthalocyanine rings are commonly employed strategies for reducing the aggregation of Pcs dyes. Accordingly, ZnPc dyes with different substituents at both the A, D sites and the B, C sites (refer to Figure 2) were conceptualized. These configurations were modeled with Gaussian 16 software to assess the impact of bulky groups on the aggregation tendencies of the ZnPc dyes. Furthermore, the torsional angles and the longest absorption wavelengths of the conceptualized ZnPc dyes were scrutinized using the Cam-B_3LYP method of the Gaussian 16 suite, utilizing the 6-311G(d) basis set, as depicted in Figure 2.[30,34] The calculation results and the simulated spectra are shown in Table S1, respectively.[35]

DFT calculations were conducted to optimize the structure of ZnPc dyes substituted by alkoxy groups with different volumes, and the results are shown in Figure 2. Based on the A and D positions as H atoms, different substituents (the vertical axial bulkiness of n-propyloxyl (2.770 Å), isopropyloxyl (3.565 Å), n-butoxy (2.783 Å), isobutoxy (4.471 Å), *tert*-butoxy (4.507 Å), 2,4-di-*tert*-butylphenoxy (9.087 Å), 2,4-di-*tert*-pentylphenoxy (9.134 Å)) were introduced to the B and C positions of phthalocyanine to get ZnPc dyes (C-1a, C-2a, C-3a, C-4a, C-5a, C-6a, C-6a, and C-7a). (Table S2) The vertical axial bulkiness of the ZnPc dyes was found to be 2.770, 4.720, 2.778, 4.786, 4.839, 9.095, and 9.134 Å, respectively. This trend can be attributed to the increasing volume of the peripheral groups, indicating that the vertical axial bulkiness of 2,4-di-*tert*-pentylphenoxy and 2,4-di*tert*-butylphenoxy is greater than that of *tert*-butoxy, which is in turn larger than isobutoxy, n-butoxy, and other alkoxy groups. Similarly, the vertical axial bulkiness of the monochloro-substituted ZnPc dyes (C-1b, C-2b, C-3b, C-4b, C-5b, C-6b, C-7b) is 2.023, 4.799, 2.164, 4.853, 4.928, 9.136, and 9.254 Å, respectively, while the trichloro-substituted ZnPc dyes (C-1c, C-2c, C-3c, C-4c, C-5c, C-6c, C-7c) exhibit values of 3.196, 5.945, 3.298, 5.998, 6.325, 10.340, and 10.480 Å, respectively. The increase in vertical axial bulkiness can be attributed to the steric effects of the different substituents. These bulkier substituents likely reduce intermolecular interactions, such as $\pi-\pi$ stacking between phthalocyanine molecules, by causing greater steric strain.

Apart from the vertical axial bulkiness of the ZnPc dyes, the effect of substituent volume on the dihedral angle, which reflects the noncoplanarity of the molecules, was also examined. The twisted angles or dihedral angles, representing the angle between the plane of the substituents and the isoindole ring plane of the phthalocyanine, were found to be >80° for ZnPc dyes substituted with phenoxy groups at the B and C positions. These values were higher than those observed for ZnPc dyes substituted with *tert*-butoxy groups, which had dihedral angles of approximately 60°. This suggests that the phenoxy substituents induce a greater noncoplanarity in the ZnPc structure compared to the *tert*-butoxy substituents. In addition, among the alkoxy-substituted ZnPc dyes, the *tert*-butoxy-substituted ZnPc dyes had greater twisted angles than the other alkoxy-substituted ZnPc dyes (~50°). This could be due to the fact that the volume of phenoxy is larger than that of *tert*-butoxy (Table S2), which is larger than that of the other alkoxy substituents, resulting in a change in the dihedral angle of the ZnPc dyes. In addition, the twist angle of the substituent planes of the monochloro-substituted ZnPc dyes (C-1b, C-2b, C-3b, C-4b, C-5b, C-6b, C-7b) are larger (~59°) than those of the nonchloro-substituted ZnPc dyes (C-1a, C-2a, C-3a, C-4a, C-5a, C-6a, C-7a) (~58°). This is because the size of the atom Cl (atomic radius 0.99 Å) adjacent to the substituent group is larger than that of H (atomic radius 0.58 Å), and the occupation of the substituent group by the larger size atoms in the neighboring positions of the phthalocyanine ring can increase the dihedral angle of phthalocyanine core, torsion angle.[32] As the dihedral angle of the ZnPc dyes increases, the noncoplanarity of the molecules also increases, resulting in a greater distance between individual molecules. The increase in molecular separation effectively reduces intermolecular interactions, such as $\pi-\pi$ stacking, between the phthalocyanine molecules.[30] As a result, the reduction in these interactions contributes to the improved solubility of the ZnPc dyes.

In addition, as shown in Figure 2, the torsion angle of ZnPc dyes (C-1a−C-7a, C-1b−C-7b) with H atoms at A and D positions are close to 1°, presenting a planar structure, while

https://doi.org/10.1021/acsomega.4c08931
ACS Omega 2024, 9, 50774−50785

Scheme 1. Synthetic Route of the Designed ZnPcs

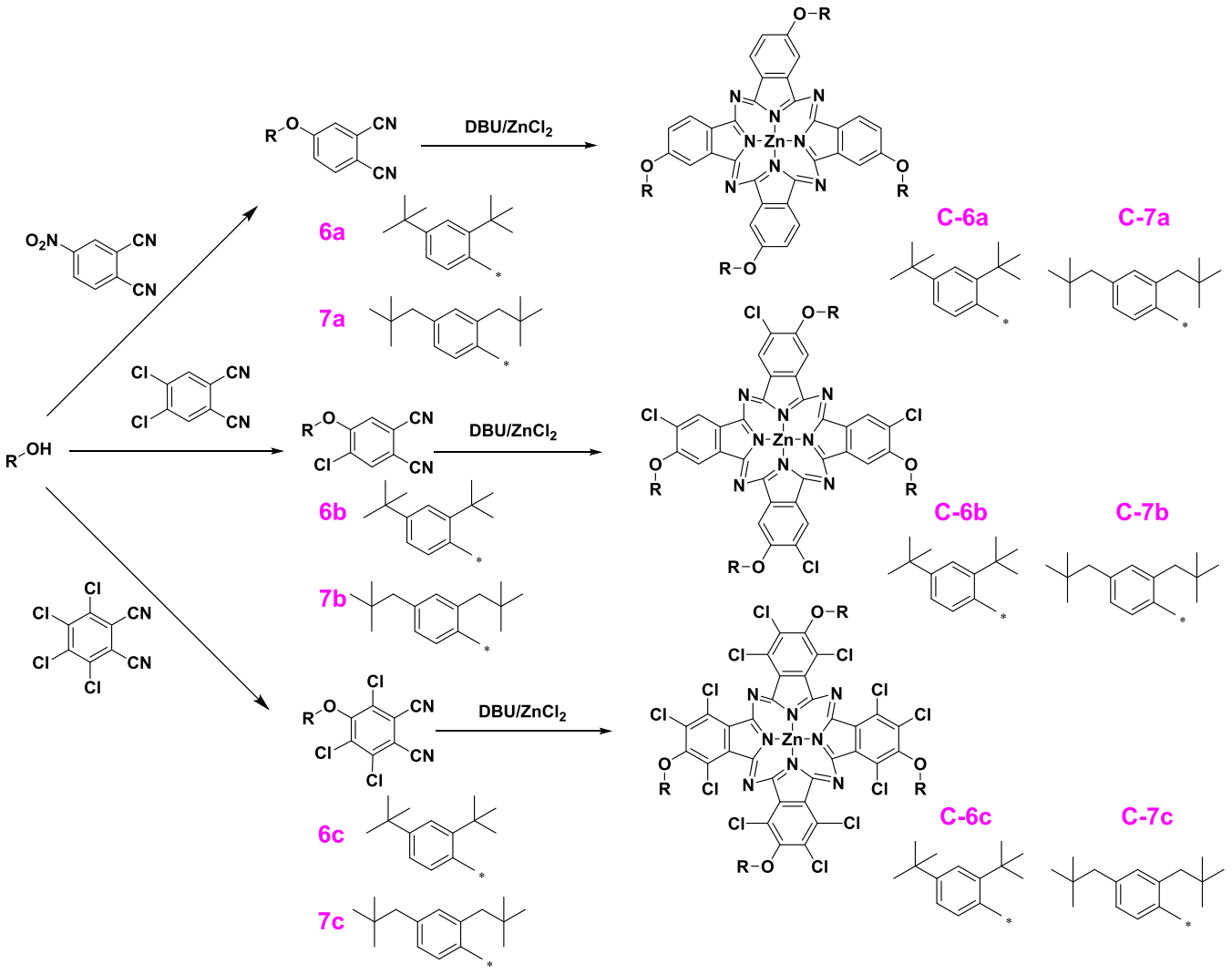

the torsion angle of ZnPc dyes C-1c−C-7c, whose A and D positions were substituted by chlorine atoms, are 9°, presenting a noncoplanar saddle structure. This is due to the repulsive effect between the neighboring Cl atoms at the A and D positions, which leads to an increase in the spatial strain and the dihedral angle of the core structure for the phthalocyanine molecule. This suggests that the substituents at the A and D positions have a significant effect on the configuration of the phthalocyanine ring. The resulting distorted structure introduces spatial separation within the ZnPcs conjugated system, which weakens the $\pi-\pi$-stacking interactions between the ZnPcs molecules. As a result, this reduction in intermolecular interactions contributes to an enhancement in the solubility of ZnPc dyes.

Furthermore, to theoretically verify the feasibility of ZnPc dyes, the maximum absorption wavelength of the designed ZnPc dyes was calculated by TD-DFT and displayed in Table S1. ZnPc dyes C-1a−C-7a and C-1b−C-7b had a similar maximum absorption wavelength (616 nm), whereas the maximum absorption wavelength of C-1c−C-7c (654 nm) was red-shifted over 30 nm. This can be attributed to the varying electron-withdrawing abilities of the substituents (σ_pCl = 0.23, σ_pH = 0) (Table S3). The introduction of chlorine (Cl) at the A and D positions of the phthalocyanine ring increases the electron density of the isoindole ring, causing the molecular configuration to transition from a planar to a distinct saddle-like structure. This structural change enhances the electron density across the entire π-conjugated system, which in turn broadens the absorption spectrum into the near-infrared region, leading to a longer absorption wavelength.

Based on the above results, representative ZnPc dyes with large dihedral angles and vertical axial bulkiness—namely C-6a, C-7a, C-6b, C-7b, C-6c, and C-7c—were chosen as candidates for synthesis and for analyzing the correlation between their structures and properties.

3.2. Synthesis, Solubility, and Absorbance Spectra of the Designed ZnPc Dyes. Six ZnPc dyes with varying volumes of sterically hindered substituents at their peripheral positions were designed and synthesized, as illustrated in Scheme 1. The synthesis of each precursor (6a, 7a, 6b, 7b, 6c, and 7c) involved a nucleophilic aromatic substitution reaction between phthalonitrile derivatives (4-nitrophthalonitrile, 3,4,5,6-tetrachlorophthalonitrile, and 4,5-dichlorophthalonitrile) and nucleophilic reagents (2,4-di*tert*-butylphenol and 2,4-di-*tert*-pentylphenol). The ZnPc dyes (C-6a, C-7a, C-6b, C-7b, C-6c, and C-7c) were subsequently synthesized through the cyclotetramerization of these precursors. All synthesized products were purified via column chromatography, yielding

https://doi.org/10.1021/acsomega.4c08931
ACS Omega 2024, 9, 50774−50785

products in the range of 60 to 90%. Comprehensive details of the structural characterization, including FTIR spectra, NMR spectra, and MALDI-TOF mass spectra, are presented in Figures S1−S30.

The solubility of the novel ZnPc dyes, which vary in the size of the sterically hindered substituents, was investigated using PGMEA as the solvent. PGMEA is commonly used as an industrial solvent in the preparation of color films.[30] The solubility results are presented in Table 1. At 25 °C, the solubilities of C-6a, C-7a, C-6b, C-7b, C-6c, and C-7c in PGMEA were found to be 7.73, 7.80, 7.81, 7.87, 8.32, and 8.40 g/100 g, respectively. This enhanced solubility can be attributed to the presence of bulky groups such as 2,4-di-*tert*-butylphenoxy and 2,4-di-*tert*-pentylphenoxy at the B and C positions of the ZnPc dyes. The significant steric hindrance and reduced planarity caused by these substituents with high vertical axial bulkiness (∼9.000 Å) contribute to the high solubility of the synthesized dyes in PGMEA. The decrease in molecular planarity and the increase in disorder hinder the packing of ZnPc molecules, which in turn enhances their solubility. Furthermore, the solubility of the ZnPc dyes in PGMEA follows the order: C-7c > C-6c > C-7b > C-6b > C-7a > C-6a. This suggests that a larger dihedral angle in the phthalocyanine structure (as shown in Table S1) corresponds to an increased solubility. The larger dihedral angle reduces intermolecular interactions, leading to lower aggregation of the ZnPc dyes.[5] In addition, the solubilities of C-7a, C-7b, and C-7c are larger than that of C-6a, C-6b, and C-6c, which is attributed to the larger vertical axial bulkiness of C-7a, C-7b, and C-7c, this is consistent with the DFT calculation results, where the torsion angle of ZnPc dyes (C-6a, C-7a, C-6b, C-7b) with H atoms at A and D positions are close to 1°, presenting a planar structure, while the torsion angle of ZnPc dyes C-6c and C-7c, whose A and D positions were substituted by chlorine atoms, are 9°, presenting a noncoplanar saddle structure. As a result, the increase in the molecular dihedral angle and vertical axial bulkiness contributes to the enhanced solubility of ZnPcs.

Table 1. Maximum Absorption Wavelength, Solubility, and Molar Extinction Coefficients of the Synthesized ZnPcs in PGMEA

ZnPc dyes	maximum absorption wavelength λ_{max} (nm)	solubility (g/100 g)	molar extinction coefficient ε_{max} ($L \cdot mol^{-1} \cdot cm^{-1}$)
C-6a	678	7.73	261,660
C-7a	678	7.80	261,300
C-6b	679	7.81	261,150
C-7b	679	7.87	260,830
C-6c	712	8.32	168,890
C-7c	712	8.40	166,760
C.I. Pigment Green 7	0	0	

The UV−visible absorption spectra of the six synthesized ZnPc dyes in PGMEA were measured at concentrations ranging from 0 to 50 $\mu mol \cdot L^{-1}$. In a previous study, the addition of DMF caused the absorbance spectra of the ZnPc dyes in PGMEA to exhibit a broad band around 740 nm, which was attributed to J-aggregated structures.[29] However, the absorbance spectra of the six ZnPc dyes in PGMEA solutions maintained their single-molecule characteristics at a concentration of 50 $\mu mol \cdot L^{-1}$ (Figures 3 and S31), suggesting that only a minimal amount of aggregation occurred in the solution. Significantly, the molar absorption coefficients of the six ZnPc dyes were determined via the Lambert−Beer law, with readings surpassing 1.6×10^5 $mol^{-1} \cdot cm^{-1}$ (refer to Table 1). This suggests that the inclusion of substituents such as 2,4-di-*tert*-butylphenol and 2,4-di-*tert*-pentylphenol not only curtailed the intermolecular clumping of phthalocyanine molecules but also maintained the high molar absorption coefficients of the dyes. The molar extinction coefficients of dyes C-6c and C-7c (∼1.6×10^5 $mol^{-1} \cdot cm^{-1}$) were lower than those of C-6a, C-7a, C-6b, and C-7b (∼2.6×10^5 $mol^{-1} \cdot cm^{-1}$), likely due to the larger dihedral angles of C-6c and C-7c.[36,37] This larger angle reduces the molecular conjugation, leading to a lower molar extinction coefficient.

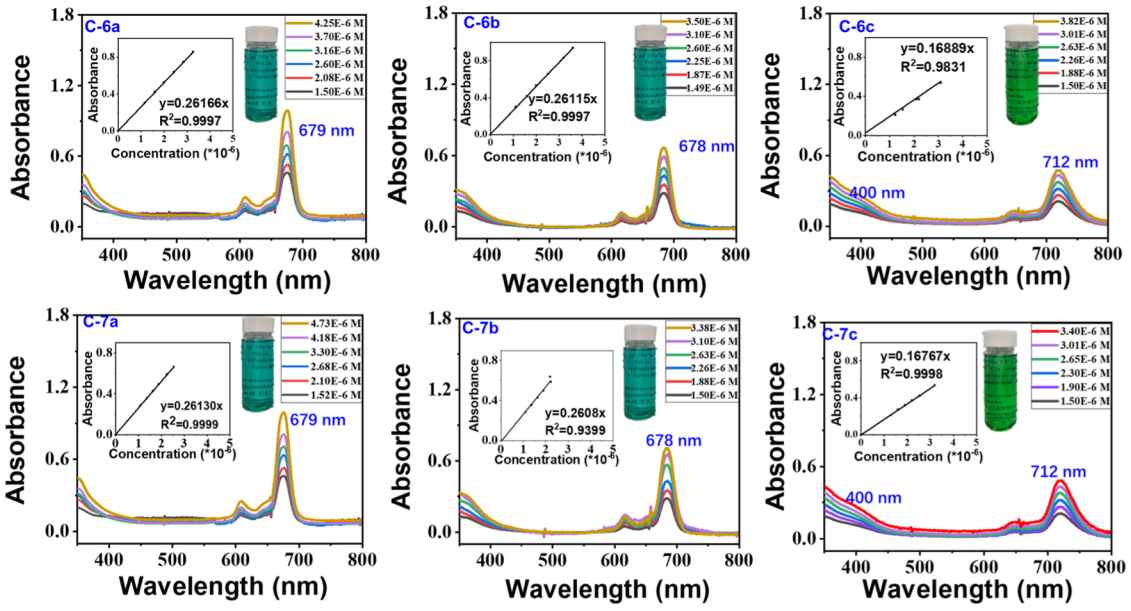

Figure 3. UV−vis absorbance spectra of the synthesized ZnPc dyes in PGMEA.

https://doi.org/10.1021/acsomega.4c08931
ACS Omega 2024, 9, 50774−50785

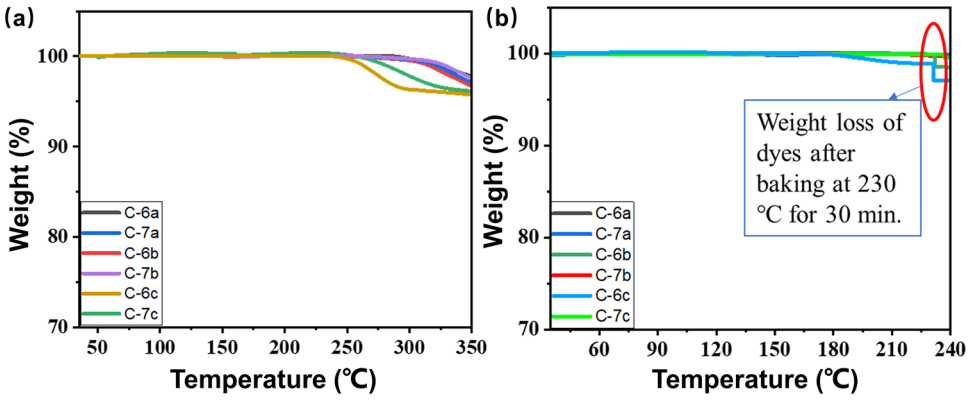

Figure 4. Thermogravimetric analysis (TGA) of the synthesized ZnPc dyes. (a) Dyes were heated to 350 °C; (b) ZnPc dyes were heated to 230 °C, maintained at that temperature for 30 min, and then further heated to 240 °C.

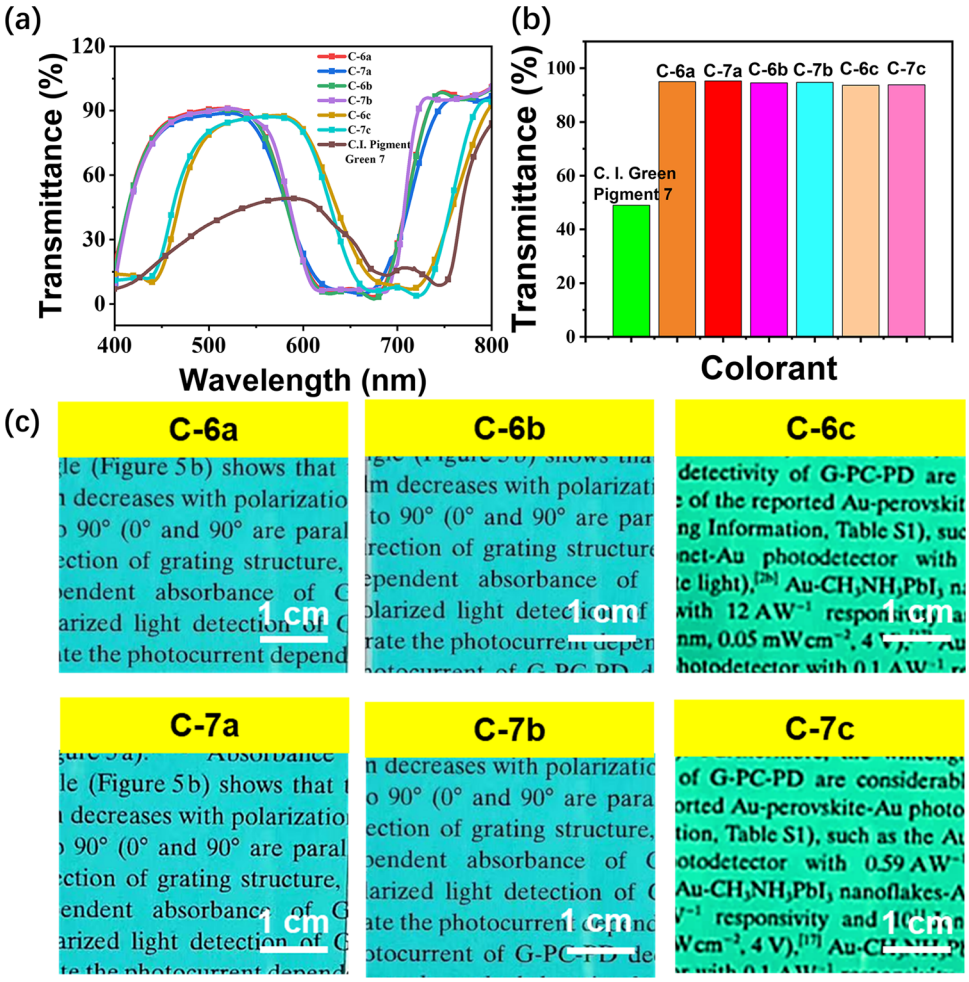

Figure 5. Characterization of the novel color films. (a) Transmittance spectra of the composite films prepared using the synthesized ZnPc dyes (C-6a, C-7a, C-6b, C-7b, C-6c, C-7c) and the commercial filter pigment (C.I. Pigment Green 7) at the same mass fraction (1.25 wt %); (b) Transmittance of the ZnPc and commercial filter pigment-based films (1.25 wt %); (c) Optical images of the C-6a, C-7a, C-6b, C-7b, C-6c, C-7c, and commercial pigment-based films (1.25 wt.%).

In order to study the photophysical properties of the synthesized ZnPc dyes, their UV−vis absorption spectra were recorded in PGMEA. As illustrated in Figure 4, all six synthesized dyes exhibit characteristic Q-band (600−720 nm) and B-band (300−400 nm) absorption spectra typical of phthalocyanines.[29] The Q-band absorption arises from $\pi \rightarrow \pi^*$ electronic transitions within the conjugated π system of the phthalocyanine ring, while the B-band absorption corresponds to higher-energy transitions, primarily attributed to $\pi \rightarrow \pi^*$ transitions involving the outer π orbitals of the phthalocyanine core. All of the synthesized dyes show maximum absorption within the 600−720 nm range, resulting in different colors of cyan and green. Among these dyes, C-6a, C-6b, C-7a, and C-7b exhibit identical maximum absorption at 678 nm, which is

https://doi.org/10.1021/acsomega.4c08931
ACS Omega 2024, 9, 50774−50785

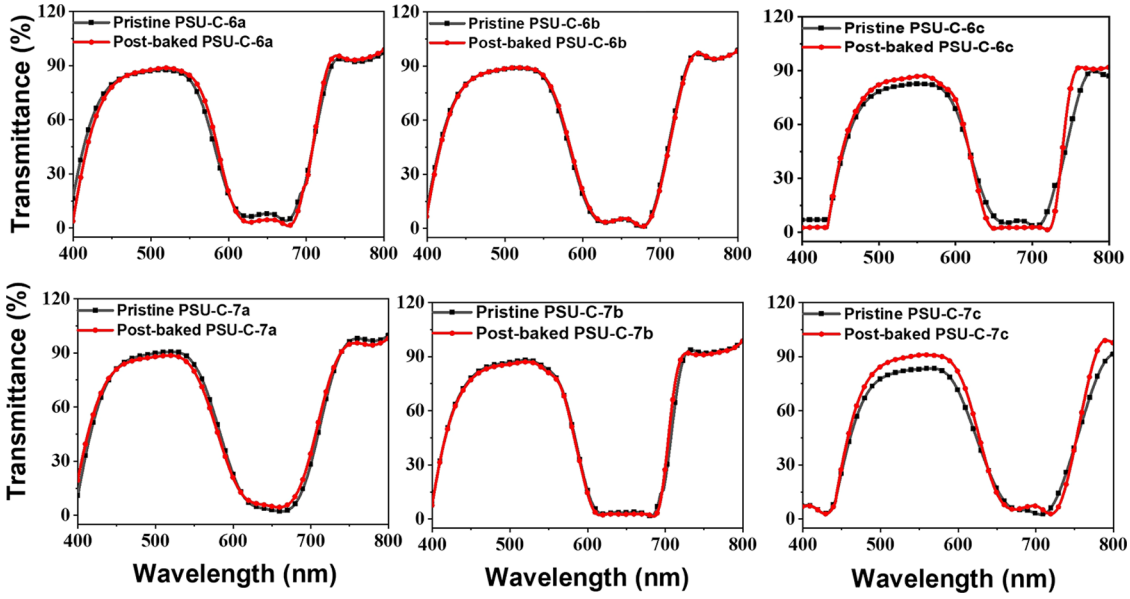

Figure 6. Transmittance spectra of six synthesized ZnPc dye-based color films before and after baking (1.25 wt %).

consistent with the time-dependent density functional theory (TD-DFT) calculation results. In dyes C-6b and C-7b, the number of substituents at the peripheral positions doubles from four to eight compared to those in dyes C-6a and C-7a. Despite this difference, the maximum absorption wavelength remains unchanged, suggesting that variations in the electron-donating power of chlorine substituents at the peripheral positions do not significantly influence the optical absorption wavelength. However, in dyes C-6c and C-7c, the Q-band absorption shifts to 712 nm, approximately 30 nm longer than that observed in dyes C-6a, C-6b, C-7a, and C-7b. This trend aligns with the TD-DFT calculations (Table S1) and is attributed to the presence of substituents at nonperipheral positions. The introduction of these substituents induces a twist in the molecular geometry, resulting in a saddle-shaped conformation.[29] This structural change alters the electron density distribution within the isoindole ring of the phthalocyanine core, leading to a reduction in the molecular absorption coefficient and a red shift in the Q-band to longer wavelengths.

3.3. Thermal Stability of the Synthesized ZnPc Dyes. For phthalocyanine dyes employed in optical instruments, ensuring both optical and thermal stabilities is crucial. To evaluate thermal stability, thermogravimetric analysis (TGA) was conducted (Figure 4), with the corresponding data presented in Table S4. The six synthesized ZnPc dyes exhibited decomposition temperatures (T_d) exceeding 230 °C (Figure 4a). This high thermal stability can be attributed to the enhanced dynamic flexibility of the alkyl chains within the molecular structure.[21] When dye molecules absorb energy and become excited, the energy of the excited state can be dissipated through the vibration and rotation of the flexible alkyl chains, which is subsequently converted into heat via internal conversion.[33] The six ZnPc dyes demonstrated excellent heat resistance, with weight losses of less than 3.0 wt %, as shown in Figure 4b. Specifically, the mass losses of C-6a, C-7a, C-6b, C-7b, C-6c, and C-7c after baking at 230 °C for 30 min were 0.15, 0.17, 0.13, 0.11, 2.70, and 2.21%, respectively (Table S4). The thermal stability of these dyes followed the order: C-7a > C-6a > C-7b > C-6b > C-7c > C-6c. This trend aligns with the dihedral angle and vertical axial length data presented in Figure 2. The more planar structures of C-6a, C-7a, C-6b, and C-7b exhibited superior stability compared with C-6c and C-7c. The higher bulkiness of the molecular structures reduces intermolecular interactions, resulting in lower crystallinity and enhanced thermal resistance.[27] As a result, the increase in molecular bulkiness may reduce the stability against thermal degradation. However, all of the prepared ZnPc dyes exhibit a mass loss of less than 5%, which satisfies the thermal stability requirements for the preparation of color film materials.[21]

3.4. Properties of the ZnPc Dye-Based Color Films. Polysulfone (PSU) with high transmittance was considered as a potential polymer binder for color films. The thermal stability of the polymer binder was investigated by TGA and DSC analyses, the curves of which are shown in Figure S32. The unaltered PSU films, which had not undergone baking, exhibited a transmission rate exceeding 90% across the wavelength spectrum from 400 to 800 nm. Furthermore, the transmission rate of the PSU films remained stable at approximately 90% even after being subjected to a baking process at 230 °C. The six ZnPc dye-derived color films that were synthesized were examined for their optical characteristics and thermal stability. C.I. Pigment Green 7 (refer to Figure S33), a readily accessible pigment frequently employed as a filter in color film applications, was chosen as a benchmark. The transmission spectra and optical microscopic images of the synthesized ZnPc dye-based color films, along with the commercial pigment film (C.I. Pigment Green 7) at a 1.25 wt % concentration, are depicted in Figure 5a–c, respectively.

The transmittance spectra and corresponding results are presented in Figure 5a,5b, demonstrating that the transmittance of ZnPc dye-based color films (>90%) was significantly higher than that of commercial pigment-based films (48%). This enhanced transmittance could be attributed to the superior dispersion characteristics of the synthesized ZnPc dyes in PSUs, compared to C.I. Green Pigment 7, which minimizes optical losses caused by scattering effects. Additionally, when the six novel color films were placed over black paper, the black characters remained visible under normal

https://doi.org/10.1021/acsomega.4c08931
ACS Omega 2024, 9, 50774−50785

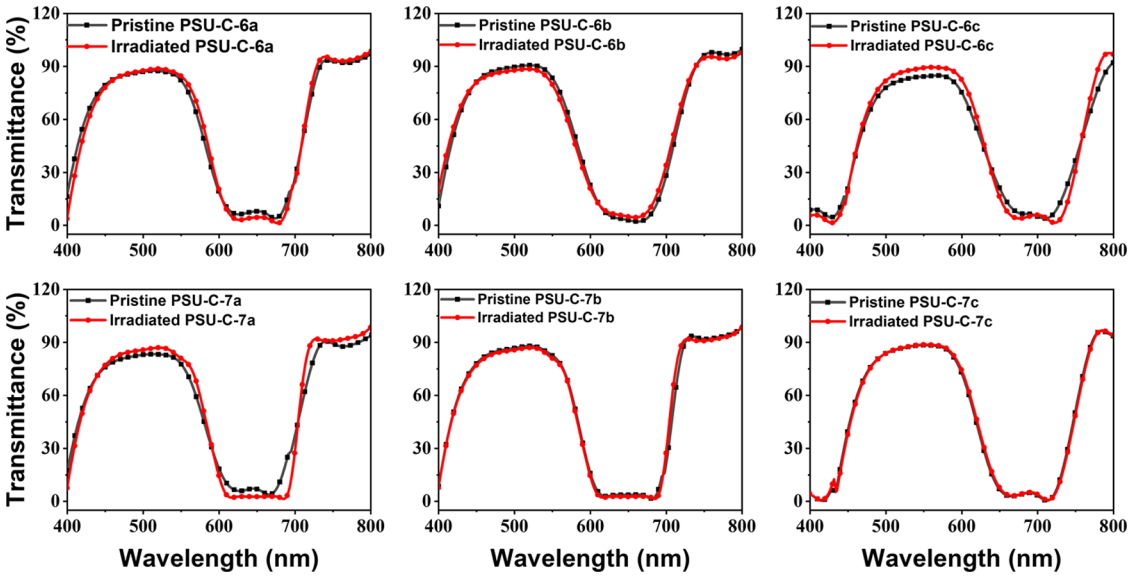

Figure 7. Transmittance spectra of six synthesized ZnPc dye-based color films before and after irradiation (1.25 wt %).

incident light, as shown in Figure 5c. These results suggest that the incorporation of substituents into phthalocyanine structures can markedly enhance the transmission properties of the color films. In order to assess thermal stability, the transmission levels of the color films were gauged both prior to and following a 30 min baking process at 230 °C. As shown in Figure 6, there was minimal change in the transmittance of the color films post baking, indicating the excellent thermal stability of the synthesized ZnPc dye-based films. This result aligns with the TGA and differential scanning calorimeter measurements, which demonstrated the high thermal decomposition temperature (T_d) and glass transition temperature (T_g) of PSU, attributed to the strong intermolecular forces induced by its stable monomeric structure.[36] The strong $\pi-\pi$ interactions between the phthalocyanine ring and its conjugated groups, the benzene ring of the substituent group, and the aromatic ring in the main chain of the PSU polymer, along with the incorporation of alkyl chains in the substituent groups, enhance the compatibility of the phthalocyanine molecules with the polymer matrix. This restricts the movement of dye molecules in the film, thereby preventing dye aggregation and improving the thermal stability of the color films.[37]

The color difference (ΔE) of the color films before and after baking was calculated to further assess their thermal stability. As shown in Table S5, the ΔE values of the six synthesized ZnPc dye-based color films are all well below 3, meeting the industrial standard requirements.[21]

Furthermore, The photostability of the six ZnPc dye-based color films that were synthesized was tested under exposure to an LED lamp emitting at a 365 nm wavelength. As illustrated in Figure 7, the transmission spectra of all six ZnPc dye-based films showed consistency, with the color difference (ΔE) staying under 3, as detailed in Table S6, even as the duration of exposure to the LED lamp increased. This minimal ΔE indicates that the films experienced negligible color changes that were imperceptible to the naked eye. Consequently, these six synthesized ZnPc dyes demonstrate high photostability comparable to commercial pigments, making them suitable for the preparation of cyan and green transparent films.[32]

4. CONCLUSIONS

In conclusion, the introduction of 2,4-di-*tert*-butylphenoxy, 2,4-di-*tert*-pentylphenoxy on the peripheral positions, along with varying numbers of chlorine atoms at the nonperipheral positions, enhances the molecular noncoplanarity and reduces the intermolecular aggregation of the zinc phthalocyanine dyes (ZnPcs). This modification results in the development of six highly soluble novel ZnPc dyes: C-6a, C-6b, C-7a, C-7b, C-6c, and C-7c, with solubility values of 7.81, 7.87, 7.73, 7.80, 8.32, and 8.40 g/100 g in PGMEA, respectively. Additionally, the variation in the number of chlorine atoms at the nonperipheral positions alters the photophysical properties of the ZnPc dyes, yielding cyan-colored dyes (C-6a, C-7b, C-6b, C-7b) and green-colored dyes (C-6c, C-7c). Additionally, the color films created with the six synthesized ZnPc dyes and PSU demonstrated remarkable photothermal stability (T_d exceeding 230 °C, color difference ΔE less than 3) under industrial production conditions. Such materials hold great potential for use in organic electronic devices.

■ ASSOCIATED CONTENT

Supporting Information

The Supporting Information is available free of charge at https://pubs.acs.org/doi/10.1021/acsomega.4c08931.

TD-DFT calculation results of the designed ZnPc dyes C-6a, C-7a, C-6b, C-7b, C-6c, and C-7c in Table S1; vertical axial bulkiness of different substituents used for peri- substitution in Table S2; Hammett constants of some substituents used for bay substitution in Table S3; FTIR spectra, ^{1}H NMR spectra, ^{13}C NMR spectra, and mass spectra of ZnPc dyes in Figures S1−S30; UV−vis absorption spectra in Figure S31; weight losses of the synthesized Pcs at 230 °C for 30 min in Table S4; thermal gravimetric analysis, differential scanning calorimeter measurements, and transmittance spectrum of PSU before and after baking in Figure S32; molecular structure and optical image of C.I. Pigment Green 7-based film in Figure S33; lab data and color difference value (ΔE) of the synthesized dye-based films before and after baking in Table S5; lab data and color

https://doi.org/10.1021/acsomega.4c08931
ACS Omega 2024, 9, 50774−50785

difference value of the synthesized dye-based films before and after accelerated irradiation in Table S6 (PDF)

AUTHOR INFORMATION

Corresponding Author

Shufen Zhang − *State Key Laboratory of Fine Chemicals, Frontier Science Center for Smart Materials, Dalian University of Technology, Dalian 116024, China;* orcid.org/0000-0003-3390-4199; Email: zhangshf@dlut.edu.cn

Authors

Shi Li − *State Key Laboratory of Fine Chemicals, Frontier Science Center for Smart Materials, Dalian University of Technology, Dalian 116024, China*

Yong Qi − *State Key Laboratory of Fine Chemicals, Frontier Science Center for Smart Materials, Dalian University of Technology, Dalian 116024, China*

Jiahui Wang − *State Key Laboratory of Fine Chemicals, Frontier Science Center for Smart Materials, Dalian University of Technology, Dalian 116024, China*

Wenbin Niu − *State Key Laboratory of Fine Chemicals, Frontier Science Center for Smart Materials, Dalian University of Technology, Dalian 116024, China;* orcid.org/0000-0001-5507-1592

Wei Ma − *State Key Laboratory of Fine Chemicals, Frontier Science Center for Smart Materials, Dalian University of Technology, Dalian 116024, China;* orcid.org/0000-0003-2283-9563

Bingtao Tang − *State Key Laboratory of Fine Chemicals, Frontier Science Center for Smart Materials, Dalian University of Technology, Dalian 116024, China;* orcid.org/0000-0001-5201-9924

Complete contact information is available at: https://pubs.acs.org/10.1021/acsomega.4c08931

Notes

The authors declare no competing financial interest.

ACKNOWLEDGMENTS

This work was supported by the Program of the National Natural Science Foundation of China (22238002), the Fundamental Research Funds for the Central Universities (DUT22LAB610), and Research and Innovation Team Project of Dalian University of Technology (DUT2022TB10).

REFERENCES

(1) Urbani, M.; Ragoussi, M. E.; Nazeeruddin, M. K.; Torres, T. Phthalocyanines for dye-sensitized solar cells. *Coord. Chem. Rev.* **2019**, *381*, 1−64.

(2) Yanık, H.; Yeşilot, S.; Durmuş, M. Synthesis and properties of octa-distyryl-BODIPY substituted zinc(II) phthalocyanines. *Dyes Pigm.* **2017**, *140*, 157−165.

(3) Torre, D. L. G.; Bottari, G.; Sekita, M.; Hausmann, A.; Guldi, M. D.; Torres, T. A voyage into the synthesis and photophysics of homo- and heterobinuclear ensembles of phthalocyanines and porphyrins. *Chem. Rev.* **2013**, *42*, 8049.

(4) Zheng, B. D.; Ye, J.; Huang, Y. Y.; Xiao, M. T. Phthalocyanine-based photoacoustic contrast agents for imaging and theranostics. *Biomater. Sci.* **2021**, *9*, 7811.

(5) Liu, Z. W.; Pan, C. Y.; Cui, J.; Wang, F. Nano phthalocyanine blue pigment dispersion with high absorption coefficient and high transparency for high chroma industrial coatings. *Prog. Org. Coat.* **2024**, *188*, No. 108253.

(6) De Riccardis, A.; Lee, M.; Kazantsev, R. V.; Garza, J. A.; Zeng, G.; Larson, M. D.; Clark, L. E.; Lobaccaro, P.; Burroughs, W. W. P.; Bloise, E.; Ager, J. W.; Bell, T. A.; Gordon, H. M.; Mele, M.; Toma, M. F. Heterogenized pyridine-substituted cobalt(II) phthalocyanine yields reduction of CO_2 by tuning the electron affinity of the Co center. *ACS Appl. Mater. Interfaces* **2020**, *12*, 5251−5258.

(7) Balamurugan, G.; Park, J. S. Enhanced solution processing and optical properties of perhalogenated zinc-phthalocyanines via anion-π bonding. *Dyes Pigm.* **2022**, *201*, No. 110199.

(8) Tubić, A.; Vujić, M.; Gvoić, V.; Ababa, J.; Vasiljevi, S.; Cveticanin, L.; Vukeli, D.; Prica, M. Sorption potential of microplastics for azo- and phthalocyanine printing dyes. *Dyes Pigm.* **2023**, *209*, No. 110884.

(9) Shang, H.; Xue, Z.; Wang, K.; Liu, H.; Jiang, J. Multinuclear Phthalocyanine-fused molecular nanoarrays: synthesis, spectroscopy, and semiconducting property. *Chem. - Eur. J.* **2017**, *23*, 8644−8651.

(10) Chakroun, R.; Jamoussi, B.; Al-Mur, B.; Timoumi, A.; Urbani, K. E. Impedance Spectroscopy and Dielectric Relaxation of Imidazole-Substituted Palladium(II) Phthalocyanine (ImPdPc) for Organic Solar Cells. *ACS Omega* **2021**, *6*, 10655−10667.

(11) Pavel, I. A.; Lasserre, A.; Simon, L.; Rossignol, J.; Lakard, S.; Stuerga, D.; Lakard, B. Microwave gas sensors based on electrodeposited polypyrrole−nickel phthalocyanine hybrid films. *Sensors* **2023**, *23*, 5550.

(12) Li, B.; Wei, P.; Leon, A.; Frey, T.; Pentzer, E. Polymer composites with photo-responsive phthalocyanine for patterning in color and fluorescence. *Eur. Polym. J.* **2017**, *89*, 399−405.

(13) Kong, S.; Wang, X.; Bai, L.; Song, Y.; Meng, F. Multi-arm ionic liquid crystals formed by pyridine-mesophase and copper phthalocyanine. *J. Mol. Liq.* **2019**, *288*, No. 111012.

(14) Halaskova, M.; Rahali, A.; Marrero, V. A.; Machacek, M.; Kucera, R.; Kucera, R.; Jamoussi, B.; Torres, T.; Novakova, V.; Escosura, A.; Zimcik, P. Peripherally crowded cationic phthalocyanines as efficient photosensitizers for photodynamic therapy. *ACS Med. Chem. Lett.* **2021**, *12*, 502−507.

(15) Valiente-Gabioud, A. A.; Miotto, M. C.; Chesta, M. E.; Lombardo, V.; Binolfi, A.; Fernánde, C. Phthalocyanines as Molecular Scaffolds to Block Disease-Associated Protein Aggregation. *Acc. Chem. Res.* **2016**, *49*, 801−808.

(16) Sakthinathan, I.; Mahendran, M.; Krishnan, K.; Karuthapandi, S. Selenium tethered copper phthalocyanine hierarchical aggregates as electrochemical hydrogen evolution catalyst. *Sustainable Energy Fuels* **2021**, *5*, 3617.

(17) Thiruppathiraja, T.; Arokiyanathan, A. L.; Aazaad, B.; Silviya, R.; Lakshmipathi, S. OH and COOH functionalized magnesium phthalocyanine as a catalyst for oxygen reduction reaction (ORR) − A DFT study. *Int. J. Hydrogen Energy* **2020**, *45*, 8540−8548.

(18) Şen, Z.; Tarakci, D. K.; Gürol, I.; Ahsen, V.; Harbeck, M. Governing the sorption and sensing properties of titanium phthalocyanines by means of axial ligands. *Sens. Actuators, B* **2016**, *229* (2016), 581−586.

(19) Namgoong, J. W.; Kim, H. M.; Kim, S. H.; Yuk, S. B.; Choi, J.; Kim, J. P. Synthesis and characterization of metal phthalocyanine bearing carboxylic acid anchoring groups for nanoparticle dispersion and their application to color filters. *Dyes Pigm.* **2021**, *184*, No. 108737.

(20) Özdemir, M.; Abliatipova, A.; Benian, S.; Yalçın, B.; Salan, U.; Durmuş, M.; Bulut, M. 1,2,3-Triazole incorporated coumarin carrying metal-free, Zn(II), Mg(II) phthalocyanines: Synthesis, characterization, theoretical studies, photophysical and photochemical properties. *J. Photochem. Photobiol., A* **2020**, *403*, No. 112845.

(21) L'Her, M.; Göktuğ, Ö.; Durmuş, M.; Ahsen, V. A. A water soluble zinc phthalocyanine: physicochemical, electrochemical studies and electropolymerization. *Electrochim. Acta* **2016**, *213*, 655−662.

(22) Gorduk, S. Highly soluble HOPEMP-functionalized phthalocyanines for photodynamic activity: Photophysical, photochemical and aggregation properties. *J. Mol. Struct.* **2020**, *1217*, No. 128478.

(23) Ovchenkova, E. N.; Bichan, N. G.; Lomova, T. N. New soluble octakis-substituted Co(II) phthalocyanines: Synthesis, spectra, supramolecular chemistry. *Dyes Pigm.* **2016**, *128*, 263−270.
(24) Namgoong, J. W.; Kim, S. H.; Chung, S. W.; Kim, Y. H.; Kwak, M. S.; Kim, J. P. Aryloxy- and chloro-substituted zinc(II) phthalocyanine dyes: Synthesis, characterization, and application for reducing the thickness of color filters. *Dyes Pigm.* **2018**, *154*, 128−136.
(25) Gorduk, S.; Avciata, O. A_3B type asymmetric metallo phthalocyanines bearing carboxylic acid and *tert*-butyl groups: Photophysical, photochemical and aggregation properties. *J. Photochem. Photobiol., A* **2024**, *449*, No. 115387.
(26) Baygu, Y.; Capan, R.; Erdogan, M.; Ozkaya, C.; Acikbas, Y.; Kabay, N.; Gök, Y. Synthesis, characterization and chemical sensor properties of a novel Zn(II) phthalocyanine containing 15-membered dioxa-dithia macrocycle moiety. *Synth. Met.* **2021**, *280*, No. 116870.
(27) Kumar, A.; Brunet, J.; Varenne, C.; Ndiaye, A.; Pauly, A. Phthalocyanines based QCM sensors for aromatic hydrocarbons monitoring: Role of metal atoms and substituents on response to toluene. *Sens. Actuators, B* **2016**, *230*, 320−329.
(28) Song, X.; Xu, R.; Yao, Q.; Tian, L.; Li, J.; Yang, B.; Chen, P.; Zhang, J.; Xin, H.; Peng, X. Cu/Zn phthalocyanine dyes with up to 40% solubility in propylene glycol monomethyl ether acetate (PGMEA) for color filters. *Dyes Pigm.* **2024**, *228*, No. 112244.
(29) Xu, R.; Yang, L.; Yang, B.; Wang, W.; Yao, Q.; Li, J.; Liu, X.; Chen, P.; Peng, X. An integrated design strategy of zinc phthalocyanine dyes for LCD dye-based color filters. *Dyes Pigm.* **2023**, *219*, No. 111562.
(30) Li, S.; Qi, Y.; Niu, W.; Wang, J.; Ma, W.; Tang, B.; Zhang, S. Low-aggregated multi-color perylene diimide derivatives and their photo-thermal stability in color films. *Dyes Pigm.* **2024**, *229*, No. 112260.
(31) Li, S.; Ye, D.; Henzen, A.; Deng, Y.; Zhou, G. Novel perylene-based organic dyes for electro-fluidic displays. *New J. Chem.* **2020**, *44*, 415.
(32) Qi, J.; Duan, X.; Liu, W.; Li, Y.; Cai, Y.; Lam, J. W. Y.; Kwok, R. T. K.; Ding, D.; Tang, B. Dragonfly-shaped near-infrared AIEgen with optimal fluorescence brightness for precise image-guided cancer surgery. *Biomaterials* **2020**, *248*, No. 120036.
(33) Yuan, L.; Lu, K.; Xia, B.; Zhang, J.; Wang, Z.; Deng, D.; Fang, J.; Zhu, L.; Wei, Z. Acceptor end-capped oligomeric conjugated molecules with broadened absorption and enhanced extinction coefficients for high-efficiency organic solar cells. *Adv. Mater.* **2016**, *28*, 5980−5985.
(34) Lu, T.; Chen, F. Multiwfn: A multifunctional wavefunction analyzer. *J. Comput. Chem.* **2012**, *33*, 580−592.
(35) Speight, J. G. *Lange's Handbook of Chemistry*, 16th ed.; McGraw-Hill: New York.
(36) Kim, H. M.; Lee, H. K.; Kim, S.; Kim, J. P. Near-infrared (NIR) absorbing films based on diimmonium dye and cyanine dye for high-performance NIR cut-off filter. *Dyes Pigm.* **2022**, *207*, No. 110702.
(37) Kim, H. M.; Lee, H. J.; Lee, H. K.; Hwang, T.; Lee, J.; Kim, S.; Kim, J. P. Binder-endowed thermal stability of diimmonium dye-based near-infrared (NIR) absorbing films. *Mater. Chem. Phys.* **2021**, *270*, No. 124773.

https://doi.org/10.1021/acsomega.4c08931
ACS Omega 2024, 9, 50774−50785